

Numerical Analysis of the Effect of Charge Transfer Coefficient (CTC) on Bubble Evolution of Polymer Electrolyte Membrane (PEM) Electrolyzer

Alhassan Salami Tijani^{1,2*}, Mohammad Amirul Akmal Mohd Najib¹,
Nabilah Hanum Mustafa¹

¹School of Mechanical Engineering, College of Engineering
Universiti Teknologi MARA, 40450 Shah Alam, Selangor, Malaysia

²Solar research institute, Universiti Teknologi MARA,
40450 Shah Alam, Selangor, Malaysia

*alhassan@uitm.edu.my

ABSTRACT

There is a growing concern on the need to enhance the current density of alkaline electrolysis without compromising reduction in efficiency. During the operation of alkaline electrolyzers, a portion of the electrode surface is covered with cloud of bubbles. The bubbles increase ohmic resistance and activation overvoltage of the electrolyte. This study aims to investigate the effect of charge transfer coefficient (CTC) on the voltage characteristics of PEM electrolyzer. Matlab was used to simulate the equations. The simulation result shows that CTC values at the anode electrode range between 0.807 and 1.035. Interestingly, at CTC of 0.5 and 0.2 for anode and cathode, the operating voltage at 1 A/cm² was observed to be 2.0 V. Also at CTC of 2 and 0.5 for anode and cathode, respectively, there was a significant drop in operating voltage up to 1.62 V with a current density of 1 A/cm², this accounts for about 27% reduction in operating voltage

Keywords: PEM Electrolyzer; Charge Transfer Coefficient (CTC); MATLAB; Mathematical Model

Introduction

There is a growing concern on the impact of conventional energy consumption on the environment [1]. For example, research shows that the recent global flood crises are caused by increased global temperature and consequence increase in sea level [2]. Therefore, there is an urgent need to address the problem caused by emissions of harmful gases to the atmosphere.

One of the solutions to address this problem is the adoption of renewable energy technology [3]. Polymer Electrolyte Membrane Water Electrolyzer (PEMWE) has the potential to solve global energy crises and address the issue of greenhouse gas emissions such as CO₂ and methane gases into the air [4]–[7]. There is a growing body of literature that recognizes the importance of numerical modelling of PEM Electrolyzer. The main challenge affecting the performance of PEM electrolyzer is the irreversibility associated with the operating voltage [8]. The main parameters constituting the operating voltage of a PEM electrolyzer are reversible voltage, diffusion overvoltage, ohmic and activation overvoltage. Convective mass transfer plays a significant role in ionic transfer, heat dissipation and distribution, and electrolyte gas bubble behaviour. The electrolyte's viscosity and flow field determine the mass (ionic) transfer, temperature distribution and bubble sizes, bubble detachment and increasing velocity, which in turn affects the current and potential distributions within the electrolysis cell [9]–[11].

A higher number of gas bubbles produced due to an increased reaction rate may hinder interaction between the electrodes and the electrolyte. Electrolyte recirculation may accelerate the bubble's departure and carry them to the collectors [12]. Electrolyte recirculation effectively avoids the production of an excess overpotential due to variations in the distribution of electrolytes within the cell. The fluid velocity in the electrolyzer will cause the removal of the gas and vapour bubbles from the electrodes. On the other hand, electrolyte recirculation will also help to disperse the heat within the electrolyte uniformly [13]–[15]. The main parameter that influences the electrochemical kinetics of the PEM electrozer is the activation overvoltage. Polarization curves are popularly known to describe the current-voltage characteristics of PEM electrolyzer, however, charge transfer coefficient (CTC) provides a better understanding of the electrode characteristics of PEM electrolyzer. This study aims to investigate the effect of operating parameters such as charge transfer coefficient (CTC) on the performance of PEM electrozer.

PEM electrolyzer mode of operation

Figure 1 shows a sample of a hydrogen production device test bench. Deionized H₂O is pre-warmed by the Marcet boiler. The water is then pumped to the anode electrode of the PEM electrolyzer. Oxygen and hydrogen gas are produced at the anode and cathode electrode respectively. Other subsystems

integrated with the PEM electrolyzer are the power supply modules, peristaltic pump, temperature control, data controllers and Marcet boiler. Figure 2 shows the details of a single-cell PEM electrolyzer system with the reactions at the electrodes.

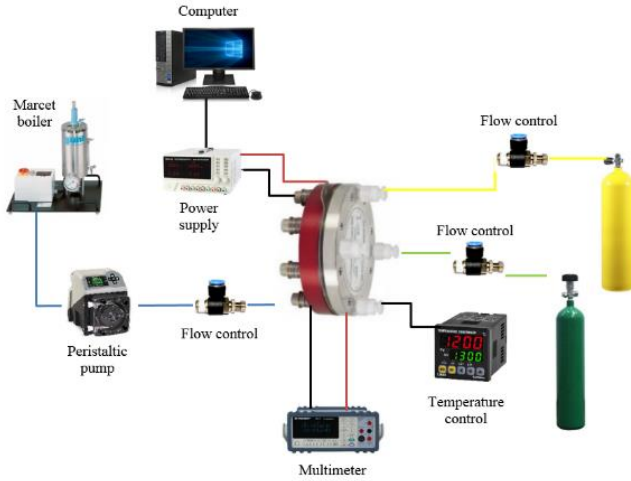


Figure 1: Components of hydrogen production system

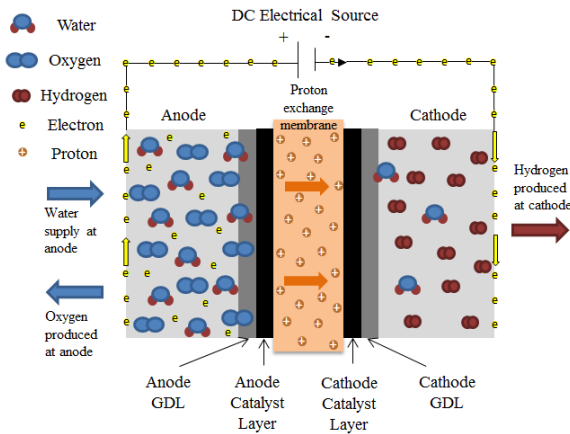
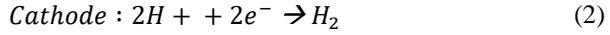
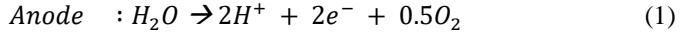


Figure 2: A PEM electrolysis cell

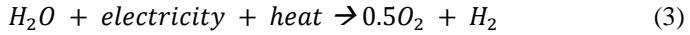
Electro-kinetics of the electrolysis

As illustrated in Equation 1, the electrical current supplied initiates the reaction kinetics at the anode electrode with the formation of positively charged

hydrogen ions. At the cathode, hydrogen gas production takes place. Detail of the reactions at the electrodes can be found in the equations below. Overall electrochemical reactions for water electrolysis is established as [16]:



Overall electrochemical reactions for water electrolysis is established as [16]:



PEM Electrolyzer Thermodynamic Modelling

Open circuit voltage

The open circuit voltage in the PEM electrolyzer is determined when there is no current flow. The Gibbs free energy is given by [17]:

$$\Delta H = \Delta G + T\Delta S \quad (4)$$

where ΔH is the theoretical enthalpy change, ΔG is the change in Gibbs free energy, T is temperature and ΔS is the change in entropy. The open circuit voltage, also known as a reversible voltage which is derived from Gibb's free Energy, is represented by [18]–[20]:

$$V_{rev} = \frac{\Delta G}{nF} \quad (5)$$

where V_{rev} is the reversible voltage, n is the number of electrons and F is a constant of Faraday. Under normal conditions $\Delta G = 237.2 \text{ kJ mol}^{-1}$, $n = 2$, $F = 96485.3 \text{ C mol}^{-1}$ and $V_{rev} = 1.23 \text{ V}$.

Activation overvoltage

Activation overvoltage is the amount of voltage needed to cause the hydrogen and oxygen atom breakup. By applying the Butler-Volmer equation, activation overpotential value can be obtained for both anode and cathode using [12] :

$$\eta_{act} = \eta_{act,a} + \eta_{act,c} \quad (6)$$

$$\eta_{act,a} = \frac{RT}{\alpha_a z_a F} \ln \left(\frac{i_a}{i_{0,a}} \right) \quad (7)$$

Charge transfer coefficient (CTC)

Charge transfer coefficient (CTC) is a limitation similar to the Butler-Volmer expression, which explains the kinetics of the electrochemical reaction in an electrolyzer. The CTC value is usually derived from the Tafel slope as:

$$\Delta V = A \log \frac{i}{i_0} \quad (8)$$

where,

$$A = \frac{RT}{2\alpha F} \quad (9)$$

At the anode side, CTC in PEM electrolyzer is significantly higher compared to the cathode as the evolution of oxygen at the anode requires a significant amount of overpotential to initiate the reaction kinetics. However, there are some literatures that treats the CTC equals to 0.5 at both electrodes. Under standard condition of simple electrochemical reactions, the CTC is assumed to be equal to the symmetric factor ($\alpha = \beta$) where $\beta = 0.5$. As for more complex reaction, the value of α is four times β , ($\alpha = 4\beta$). The list of constant parameters adopted for the simulation and validation in this study can be found in Table 1.

Table 1: Constant parameters involved in the study

Symbol	Parameter	Value	Reference
T	Temperature (K)	293 - 363	[21]
P	Pressure (bar)	1 - 20	[21]
α_A, α_C	Anode and Cathode charge transfer coefficient	0.5 - 2	[22]
R_{ele}	Electric resistance (m Ω)	0.035	[23]
z_a, z_c	Stoichiometric coefficient of electron transfer	4, 2	[21]
$i_{o,an}$	Exchange current density with Pt-Ir anode catalyst (A/cm ²)	1.0×10^{-9}	[24]
$i_{o,cat}$	Exchange current density with Pt catalyst cathode (A/cm ²)	1.0×10^{-3}	[24]
i	Current Density (A/cm ²)	0.01 – 2.0	[21]
R	Universal gas constant (J/mol K)	8.314	[22]
λ	Water humidification factor	24	[23]
σ	Membrane thickness (μ m)	178	[23]
F	Faraday constant (A/mol)	96485.3	[22]

Hydrogen production

Hydrogen production rate, V_H (ml min⁻¹) is expressed in term of input current I (A) as:

$$v_H = v_M(l) \left(\frac{10^3 ml}{1l} \right) \left(\frac{60s}{min} \right) \left(\frac{I \left(\frac{C}{s} \right)}{2F(C)} \right) = v_M(10^3)(60) \frac{I}{2F} \quad (10)$$

Input electrical power

The input electrical power to the PEM electrolyzer system is associated with input current and voltage and can be written as:

$$\begin{aligned} P = IV &= IV_{rev} + I^2 R_{ohm} + I^2 R_{act} \quad (11) \\ &= \left(\frac{v_H 2F}{v_M 10^3 (60)} \right) V_{rev} + \left(\frac{v_H 2F}{v_M 10^3 (60)} \right)^2 (R_{el} + R_{ion}) \\ &+ \left(\frac{v_H 2F}{v_M 10^3 (60)} \right)^2 \left(\frac{RT}{\alpha_a z F} \ln \left(\frac{1}{i_{o,a}} \right) + \frac{RT}{\alpha_c z F} \ln \left(\frac{1}{i_{o,c}} \right) \right) \end{aligned}$$

Assuming the resistance due to diffusion is negligible.

Efficiency

The efficiency of the PEM electrolyzer η_e with respect to the input electrical power and the useful Energy is expressed as:

$$\eta_e = \frac{P_{H_2}}{P} = \frac{V_{rev} I}{VI} = \frac{V_{rev}}{V} \quad (12)$$

Bubble evolution effect on the voltage

Bubbles attached to the electrode surface separate and inactive the covered fraction of the surface from the reacting species. This effect can be included in the re-scaling of the region leading to the current density in Equations (13) and (14), providing an additional contribution to the over-potential due to the coverage of the bubble [25]:

$$\eta_{act,a} = \frac{RT}{\alpha_a z_a F} \ln \left(\frac{i_a}{i_{o,a}} \right) + \frac{RT}{\alpha_a z_a F} \ln \left(\frac{1}{1 - \Theta_a} \right) \quad (13)$$

$$\eta_{act,c} = \frac{RT}{\alpha_c z_c F} \ln \left(\frac{i_c}{i_{o,c}} \right) + \frac{RT}{\alpha_c z_c F} \ln \left(\frac{1}{1 - \Theta_c} \right) \quad (14)$$

Result and Discussion

Validation of model

To validate the accuracy operating parameters used in this simulation, the data produced from the simulation has been compared with the experimental data from [18] using the same operating parameters and geometrical values conditions. It can be concluded from Figure 3 that the I-V characteristic of the simulation model agrees with the literature's experimental results.

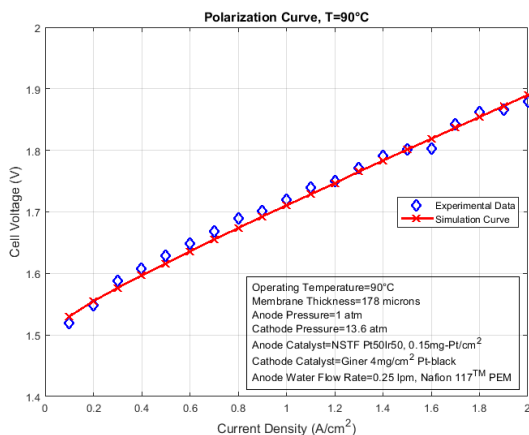


Figure 3: Effect of operating pressure on cell voltage

Temperature effect on operating voltage

Figure 4 shows the influence of temperature on the polarization curve with current densities from 0 A/cm² to 2 A/cm². The overall operating voltage declines as the working temperature rises from 30 °C to 90 °C, leading to better cell efficiency. The explanation is that electrochemical reactions are faster as the temperature rises, which increases the exchange current density and hence a reduction in loss of voltage. Figure 4b shows that, there is a significant reduction in activation overvoltage at higher temperatures. This is because the electro kinetics of the reaction at the electrodes is enhanced at higher temperatures. Figure 4c also shows a tremendous reduction in ohmic overvoltage at higher temperature.

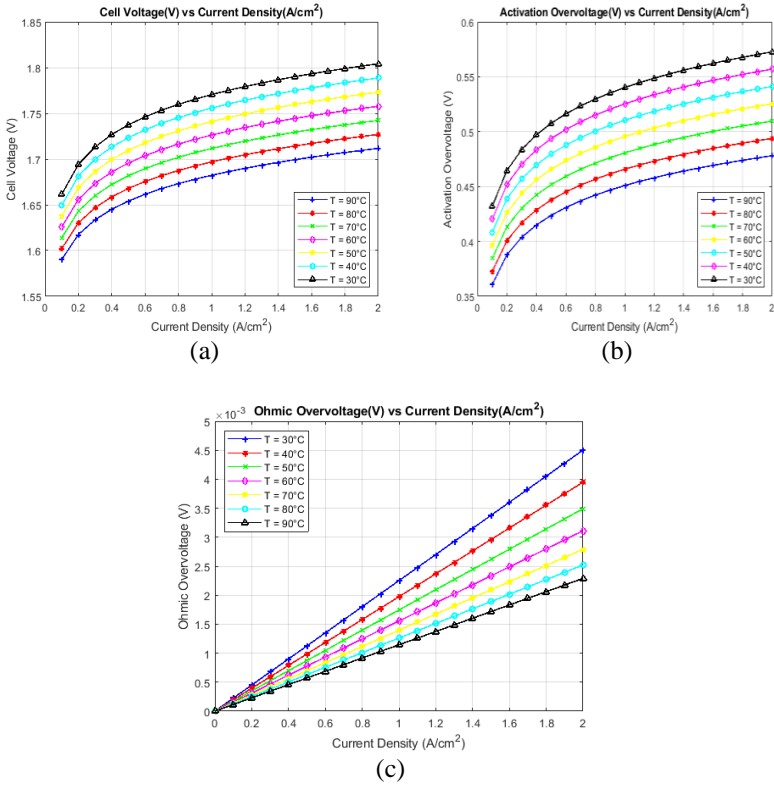


Figure 4: Effects of different operating temperature on the voltages of PEM electrolyzer; a) cell voltage, b) activation overvoltage, c) Ohmic overvoltage

Activation overpotential variation with charge transfer coefficient (CTC)

The effect of CTC variation on activation overpotential is provided in Figures 5a, 5b, and 5c. Generally, the activation overvoltage decreases when the CTC increases for all the cases tested. For example, Figure 5b indicates that 1.5 V is the maximum activation overvoltage obtained for the anode and cathode at CTC of 0.1 and this decreases sharply with the rise in CTC. The explanation is that the CTC is the fraction of the potential energy added to an electrochemical reaction that increases the rate of reaction, so the electrokinetics of the reaction at the electrodes needs less activation overpotential if CTC is increased. We can also observe from Figures 5b and 6c that the temperature also significantly influences the activation overpotential.

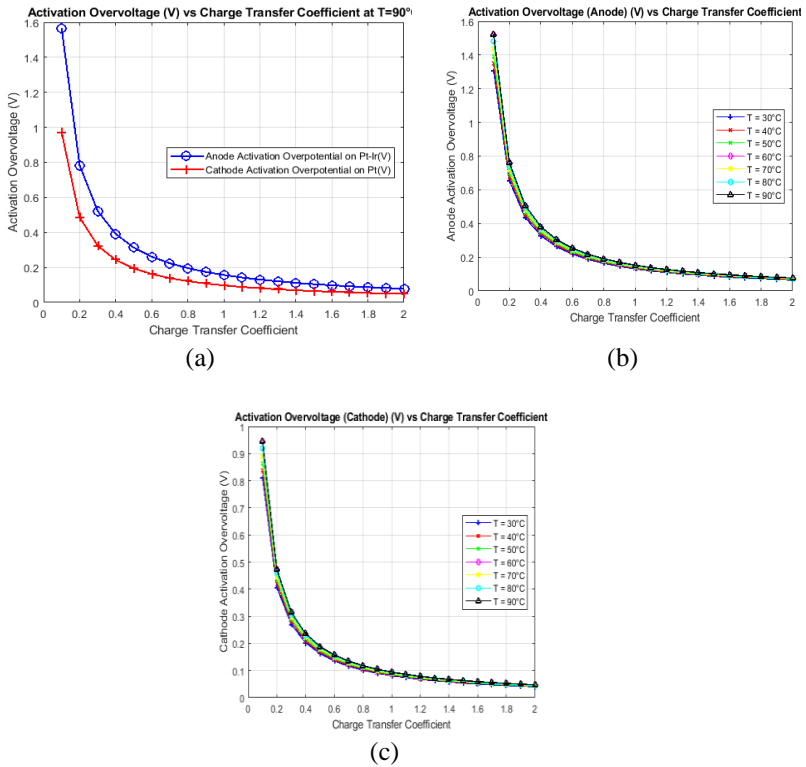


Figure 5: Activation overpotential variations with charge transfer coefficient; a) anode and cathode at T = 90 °C, b) anode activation overvoltage, c) cathode activation overvoltage

Operating pressure effect on charge transfer coefficient (CTC)

It can be observed from Figure 6a to 6e, that the cathode CTC rises just from 0.2 to 0.25 as the temperature increases from 30b °C to 90b °C. Higher CTC is required at the anode due to the electrochemical splitting of the water molecules at the anode. On the other hand, the reaction at the cathode does not require higher effort for the reaction between the cathode species (H+ and electron). Subsequently, comparative with that of the anode, the CTC at the cathode is lower.

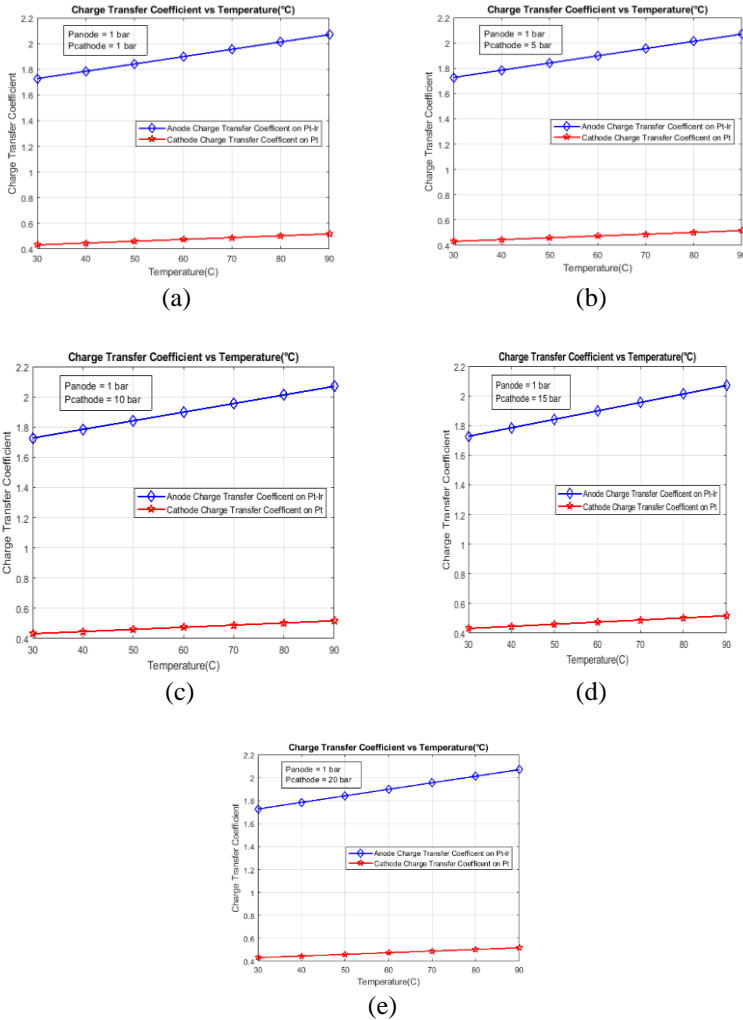


Figure 6: Different pressure effects at cathode on CTC

Fractional bubble coverage effect on the activation overvoltage

Figure 7a to 7c shows the impact of the electrode's fractional bubble coverage on the electrolyser's activation overpotential. It can be observed from the graph that as the fractional bubble coverage increase, the activation overvoltage at both anode and cathode also increases. Both anode and cathode activation overvoltage gradually increase at temperatures 30 °C and 60 °C with both voltage differences of 0.06 V and 0.11 V, respectively. The voltage differences

of anode and cathode are the smallest at 90 °C which is 0.04 and 0.067 V, respectively. This is expected because, at higher operating temperature, the activation overvoltage decreases as the electro-kinetics of water is enhanced, leading to faster reactions.

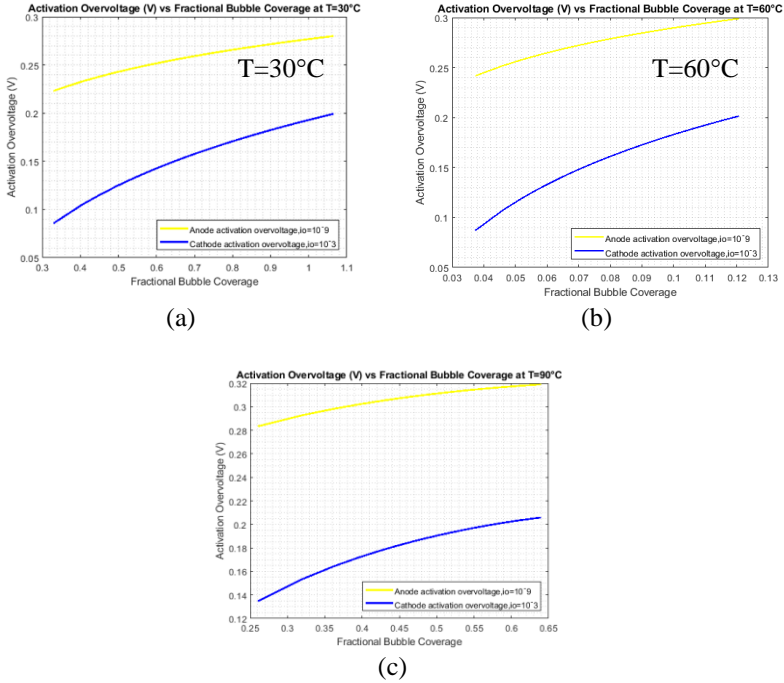


Figure 8: Fractional bubble coverage at anode and cathode with operating temperature (a) T=30 °C, (b) T=60 °C, (c) T=90 °C

Conclusion

The effect of the operating temperature and operating voltage on the Charge Transfer Coefficient (CTC) was calculated in this investigation. This study reveals that as the operating temperature of the PEM electrolyzer increases, the CTC values also increase, but they are more critical at the anode compared to cathode electrodes. Interestingly, as the CTC increases at both anode and cathode electrodes, the value of activation overvoltage declines. This has shown that CTC is highly temperature dependent and this CTC variation has an effect on the overvoltage of the electrolyzer activation. It can be concluded from this study that activation overvoltage is the main parameter that

significantly affect the operating voltage. The optimization of the operating temperature is very important.

Acknowledgement

The authors wish to thank the School of Mechanical Engineering, College of Engineering Universiti Teknologi MARA (UiTM) for providing financial and technical support.

References

- [1] C. Minke, M. Suermann, B. Bensmann, and R. Hanke-Rauschenbach, “Is iridium demand a potential bottleneck in the realization of large-scale PEM water electrolysis?,” *Int. J. Hydrogen Energy*, vol. 46, no. 46, pp. 23581–23590, 2021, doi: 10.1016/j.ijhydene.2021.04.174.
- [2] A. S. Tijani and A. H. A. Rahim, “Numerical Modeling the Effect of Operating Variables on Faraday Efficiency in PEM Electrolyzer,” *Procedia Technol.*, vol. 26, pp. 419–427, 2016, doi: 10.1016/j.protcy.2016.08.054.
- [3] F. Aubras *et al.*, “Dimensionless approach of a polymer electrolyte membrane water electrolysis: Advanced analytical modelling,” *J. Power Sources*, vol. 481, no. August 2020, p. 228858, 2021, doi: 10.1016/j.jpowsour.2020.228858.
- [4] H. Lee, B. Lee, M. Byun, and H. Lim, “Economic and environmental analysis for PEM water electrolysis based on replacement moment and renewable electricity resources,” *Energy Convers. Manag.*, vol. 224, no. September, p. 113477, 2020, doi: 10.1016/j.enconman.2020.113477.
- [5] A. Cernat, C. Pana, N. Negurescu, G. Lazaroiu, C. Nutu, and D. Fuioreescu, “Hydrogen—an alternative fuel for automotive diesel engines used in transportation,” *Sustain.*, vol. 12, no. 22, pp. 1–21, 2020, doi: 10.3390/su12229321.
- [6] F. Scheepers *et al.*, “Temperature optimization for improving polymer electrolyte membrane-water electrolysis system efficiency,” *Appl. Energy*, vol. 283, no. December 2020, pp. 1–11, 2021, doi: 10.1016/j.apenergy.2020.116270.
- [7] F. Z. Aouali, M. Becherif, H. S. Ramadan, M. Emziane, A. Khellaf, and K. Mohammedi, “Analytical modelling and experimental validation of proton exchange membrane electrolyser for hydrogen production,” *Int. J. Hydrogen Energy*, vol. 42, no. 2, pp. 1366–1374, 2017, doi: 10.1016/j.ijhydene.2016.03.101.
- [8] S. S. Lafmejani, M. Müller, A. C. Olesen, and S. K. Kær, “Experimental and numerical study of flow in expanded metal plate for water electrolysis

- applications,” *J. Power Sources*, vol. 397, no. February, pp. 334–342, 2018, doi: 10.1016/j.jpowsour.2018.07.032.
- [9] N. Rojas *et al.*, “Coated stainless steels evaluation for bipolar plates in PEM water electrolysis conditions,” *Int. J. Hydrogen Energy*, vol. 46, no. 51, pp. 25929–25943, 2021, doi: 10.1016/j.ijhydene.2021.03.100.
- [10] N. Lümme, A. Karouach, and S. Tveitan, “Thermo-economic study of waste heat recovery from condensing steam for hydrogen production by PEM electrolysis,” *Energy Convers. Manag.*, vol. 185, no. January, pp. 21–34, 2019, doi: 10.1016/j.enconman.2019.01.095.
- [11] Á. Hernández-Gómez, V. Ramirez, and D. Guilbert, “Investigation of PEM electrolyzer modeling: Electrical domain, efficiency, and specific energy consumption,” *Int. J. Hydrogen Energy*, vol. 45, no. 29, pp. 14625–14639, 2020, doi: 10.1016/j.ijhydene.2020.03.195.
- [12] M. Upadhyay *et al.*, “Three-dimensional CFD simulation of proton exchange membrane water electrolyser: Performance assessment under different condition,” *Appl. Energy*, vol. 306, no. PA, p. 118016, 2022, doi: 10.1016/j.apenergy.2021.118016.
- [13] D. S. Falcão and A. M. F. R. Pinto, “A review on PEM electrolyzer modelling: Guidelines for beginners,” *J. Clean. Prod.*, vol. 261, 2020, doi: 10.1016/j.jclepro.2020.121184.
- [14] Z. Kang *et al.*, “Performance Modeling and Current Mapping of Proton Exchange Membrane Electrolyzer Cells with Novel Thin/Tunable Liquid/Gas Diffusion Layers,” *Electrochim. Acta*, vol. 255, pp. 405–416, 2017, doi: 10.1016/j.electacta.2017.09.170.
- [15] M. S. Khan, V. Hegde, and G. Shankar, “Effect of Temperature on Performance of Solar Panels-Analysis,” *Int. Conf. Curr. Trends Comput. Electr. Electron. Commun. CTCEEC 2017*, vol. 31, no. 5, pp. 109–113, 2018, doi: 10.1109/CTCEEC.2017.8455109.
- [16] P. Olivier, C. Bourasseau, and B. Bouamama, “Modelling, simulation and analysis of a PEM electrolysis system,” *IFAC-PapersOnLine*, vol. 49, no. 12, pp. 1014–1019, 2016, doi: 10.1016/j.ifacol.2016.07.575.
- [17] A. H. A. Rahim and A. S. Tijani, “Modeling and Analysis the Effects of Temperature and Pressure on the Gas-Crossover in Polymer Electrolyte Membrane Electrolyzer,” vol. 2, no. 1, pp. 1–7, 2016.
- [18] S. Sebbahi, N. Nabil, A. Alaoui-belghiti, S. Laasri, and S. Rachidi, “Materials Today : Proceedings Assessment of the three most developed water electrolysis technologies : Alkaline Water Electrolysis , Proton Exchange Membrane and Solid-Oxide Electrolysis,” *Mater. Today Proc.*, no. xxxx, 2022, doi: 10.1016/j.matpr.2022.04.264.
- [19] J. T. H. Kwan, A. Nouri-Khorasani, A. Bonakdarpour, D. G. McClement, G. Afonso, and D. Wilkinson, “Frequency Analysis of Water Electrolysis Current Fluctuations in a PEM Flow Cell: Insights into Bubble Nucleation and Detachment,” *J. Electrochem. Soc.*, 2022, doi: 10.1149/1945-7111/ac707f.

- [20] X. Su, L. Xu, and B. Hu, "ScienceDirect Simulation of proton exchange membrane electrolyzer : Influence of bubble covering," *Int. J. Hydrogen Energy*, vol. 47, no. 46, pp. 20027–20039, 2022, doi: 10.1016/j.ijhydene.2022.04.154.
- [21] A. S. Tijani, M. F. A. Ghani, A. H. A. Rahim, I. K. Muritala, and F. A. Binti Mazlan, "Electrochemical characteristics of (PEM) electrolyzer under influence of charge transfer coefficient," *Int. J. Hydrogen Energy*, vol. 44, no. 50, pp. 27177–27189, 2019, doi: 10.1016/j.ijhydene.2019.08.188.
- [22] A. S. Tijani, N. A. Binti Kamarudin, and F. A. Binti Mazlan, "Investigation of the effect of charge transfer coefficient (CTC) on the operating voltage of polymer electrolyte membrane (PEM) electrolyzer," *Int. J. Hydrogen Energy*, vol. 43, no. 19, pp. 9119–9132, 2018, doi: 10.1016/j.ijhydene.2018.03.111.
- [23] A. S. Tijani, N. A. B. Yusup, and A. H. A. Rahim, "Mathematical Modelling and Simulation Analysis of Advanced Alkaline Electrolyzer System for Hydrogen Production," *Procedia Technol.*, vol. 15, pp. 798–806, 2014, doi: 10.1016/j.protcy.2014.09.053.
- [24] F. Marangio, M. Santarelli, and M. Cali, "Theoretical model and experimental analysis of a high pressure PEM water electrolyser for hydrogen production," *Int. J. Hydrogen Energy*, vol. 34, no. 3, pp. 1143–1158, 2009, doi: 10.1016/j.ijhydene.2008.11.083.
- [25] Z. Abdin, C. J. Webb, and E. M. A. Gray, "Modelling and simulation of an alkaline electrolyser cell," *Energy*, vol. 138, no. 2017, pp. 316–331, 2017, doi: 10.1016/j.energy.2017.07.053.